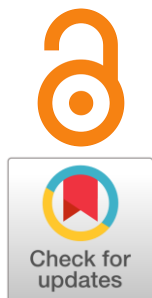# Approaches for the preparation of dense ceramics and sintering aids for Sr/Mg doped lanthanum gallate: focus review

Egor Gordeev [a] [*], Natalia Porotnikova [a] [*]

This review focuses on Sr/Mg doped lanthanum gallate and its use as a dense electrolyte for medium-temperature solid oxide electrochemical devices. Methods for synthesizing the material are discussed, including techniques that lower the temperature required to attain a single-phase crystalline structure. The effects of secondary phases and grain size on conductivity of ceramics are also investigated. Moreover, the techniques used for compacting electrolyte powder and reducing energy expenses, as well as the impacts of sintering aids on ceramic properties, are analyzed. The potential advantages and disadvantages of the proposed alterations to generate an electrolyte from doped lanthanum gallate are evaluated.

keywords: lanthanum gallate, synthesis, methods, sintering aids, ceramic compacting

1. Introduction

The worldwide need for sustainable and renewable energy sources has become a serious problem that many countries are trying to solve. In recent decades, researchers have focused on a new method to meet these requirements, which involves the development of sustainable solid oxide fuel cells. Subsequent advancements in this field have been very encouraging [1–4]. Several global companies are working to commercialize solid oxide fuel cell technology, while various research programs aim to improve our understanding of these systems and pave the way for future advances in the field.

The perovskite-like material Sr/Mg doped $LaGaO_3$

a: Institute of High–Temperature Electrochemistry, Yekaterinburg 620066, Russia
*   Corresponding author: e.gordeev@ihte.ru ; porotnikova@ihte.ru

(LSGM) is a promising candidate as an electrolyte material for solid oxide fuel cells due to its high oxygen ionic conductivity in the intermediate temperature range of 500–800 °C [5–7]. One of the highest oxygen-ion conductivities for $La_{1-x}Sr_xGa_{1-y}Mg_yO_{3-\delta}$ is observed at $x = 0.10–0.20$ and $y = 0.15–0.20$ [8–10]. The ionic conductivity of $La_{0.9}Sr_{0.1}Ga_{0.8}Mg_{0.2}O_{3-\delta}$ at 800 °C varies in the range of 0.05 to 0.11 S/cm depending on the specific synthesis method used, which affects the microstructural properties of the ceramic material [11, 12]. In addition, lanthanum gallate has the advantage of stability over a wide range of oxygen pressures with predominant ionic conductivity [13–15], and a high thermal expansion coefficient (TEC) compared to other types of electrolytes, Table 1.

Doped lanthanum gallate is a suitable electrolyte material due to its high thermal expansion coefficient over a wide temperature range, which is advantageous for compatibility with electrode materials. LSGM has a slightly lower TEC value ($11.4 \cdot 10^{-6}$ K^{-1}), compared to

Table 1 – Thermal expansion coefficients of different electrolytes.

Electrolyte	T, °C	TEC, K^{-1}	Ref
$La_{0.9}Sr_{0.1}Ga_{0.8}Mg_{0.2}O_{3-\delta}$	200–1200	$11.4 \cdot 10^{-6}$	[16, 17]
$ZrO_2-(3–10\ mol\ \%)\ Y_2O_3$	25–1000	$10.3–10.8 \cdot 10^{-6}$	[18]
$BaCe_{0.8}Y_{0.2}O_{3-\delta}$	50–620	$11.6 \cdot 10^{-6}$	[19]
	620–900	$8.3 \cdot 10^{-6}$	
$BaCe_{0.9}Gd_{0.1}Cu_{0.01}O_{3-\delta}$	100–575	$10.5 \cdot 10^{-6}$	[20]
	575–900	$8.6 \cdot 10^{-6}$	
$Ce_{0.8}Gd_{0.2}O_{2-\delta}$	20–800	$12.5 \cdot 10^{-6}$	[21]

cerium-gadolinium oxide ($12.5 \cdot 10^{-6}\ K^{-1}$). LSGM has an advantage due to the stability of its TEC value compared to barium cerates, such as $BaCe_{0.9}Gd_{0.1}Cu_{0.01}O_{3-\delta}$ and $BaCe_{0.8}Y_{0.2}O_{3-\delta}$.

The LSGM electrolyte obtained by the solid-phase method exhibits an oxygen-ionic conductivity of about 0.08 S/cm at 800 °C [11], which is two-fold higher than the conductivity of 9 mol % $Y_2O_3-ZrO_2$ (0.047 S/cm at 800 °C [22]) and three-fold higher than that for $Ce_{0.8}Sm_{0.2}O_{2-\delta}$ (0.027 S/cm at 800 °C [23]). According to Steele B.C.H. [24], the ionic conductivity of $Ce_{0.8}Gd_{0.2}O_{2-\delta}$ is 0.09 S/cm, which is comparable to LSGM electrolyte. Doped $LaGaO_3$ has a significant advantage at low oxygen partial pressures compared to cerium-containing electrolytes, namely stability under these conditions. There are limitations in the use of the LSGM electrolyte due to the chemical instability of the composition in contact with some electrode materials, which leads to interdiffusion or chemical reaction with metal components at the interface. This requires a careful choice of compositions or the use of barrier layers.

Solid oxide fuel cell components can be formed as a multilayer element for co-sintering to simplify the fabrication process and reduce production costs. However, there are technological features that prevent this process. These features relate to differences in the microstructure of the ceramic electrode layers and the electrolyte, with the former having a porous structure and the electrolyte having a dense microstructure. In addition, different types of materials have to be sintered at different temperatures, which can lead to shrinkage and chemical reactions. In the case of

$La_{0.9}Sr_{0.1}Ga_{0.8}Mg_{0.2}O_{3-\delta}$ perovskite, the main phase can be obtained at 1250 °C with a small amount of $LaSrGaO_4$ using a conventional solid phase reaction [11]. By increasing the annealing temperature to 1400 °C, a pure phase with a relative density of up to 98 % can be obtained. It is important to note that depending on the ratio of A/B cations in $La_{1-x}Sr_xGa_{1-y}Mg_yO_{3-\delta}$ and the concentration of dopants $x = y = 0$, 0.1, and 0.2, secondary phases Ga_2O_3, $(Sr,La)_2Ga_3O_7$, $(Sr,La)_2GaO_4$, $La_4Ga_2O_9$, and La_4SrO_7 are identified at the final ceramic formation temperature up to 1500 °C [25, 26].

There are inconsistent data in the literature regarding the influence of secondary phases on the total conductivity of LSGM electrolytes. At a synthesis temperature of 1400 °C, Cristiani et al. [27] obtained $La_{0.8}Sr_{0.2}Ga_{0.8}Mg_{0.2}O_{3-\delta}$, which contains the secondary phases $LaSrGaO_4$ (16 %) and $LaSrGa_3O_7$ (1 %). The value of the total conductivity of this composition ($La_{0.8}Sr_{0.2}Ga_{0.8}Mg_{0.2}O_{3-\delta}$ with $LaSrGaO_4$ and $LaSrGa_3O_7$) is 0.077 S/cm at 800 °C, which is close to the conductivity of the pure LSGM materials. According to the authors, the presence of the secondary phases $LaSrGaO_4$ and $LaSrGa_3O_7$ does not strongly influence on the electrical properties of the electrolyte layer. However, this view is challenged by alternative studies. It is well known [28, 29] that the total conductivity of melilite-type ceramics $La_{1+x}Sr_{1-x}Ga_3O_{7-\delta}$ ($x = 0–0.45$) is highly dependent on the strontium concentration. Thus, for $La_{1.45}Sr_{0.55}Ga_3O_{7-\delta}$, the value of the total conductivity is of about 0.045 S/cm at 800 °C in air, which is close to the conductivity of $La_{0.8}Sr_{0.2}Ga_{0.8}Mg_{0.2}O_{3-\delta}$. The conductivity of the $La_{1+x}Sr_{1-x}Ga_3O_{7-\delta}$ material at 800 °C decreases from $3 \cdot 10^{-5}$ to $3 \cdot 10^{-6}$ S/cm with increasing strontium concentration from $x = 0$ to $x = -0.15$, respectively [28]. The total conductivity of $LaSrGaO_4$ and $La_4Ga_2O_9$ oxides is $10^{-4}–10^{-5}$ S/cm at 800 °C, which is 3–4 times lower than that of LSGM electrolyte [30–32]. Consequently, the materials $LaSrGa_3O_7$, $La_4Ga_2O_9$, and $LaSrGaO_4$ have rather low ionic conductivity; their presence in the composition should negatively affect the ion transport of lanthanum gallate. This conclusion is supported by the results of Li et al. [33], who found that the presence of $LaSrGa_3O_7$ (2.3 %) and $LaSrGaO_4$ (2.3 %) phases in $La_{0.8}Sr_{0.2}Ga_{0.83}Mg_{0.17}O_{3-\delta}$ ceramics leads to a decrease in conductivity at 800 °C from $8.24 \cdot 10^{-2}$ S/cm for the pure material to $1.28 \cdot 10^{-3}$ S/cm with impurities. Zhang et al. [34] demonstrate a twofold decrease in the conductivity of ceramics from $3.95 \cdot 10^{-2}$ to $1.43 \cdot 10^{-2}$ S/cm in the presence of about 8 % of $LaSrGaO_4$ and $LaSrGa_3O_7$ impurity phases. The authors

also note that the effect of decreased conductivity is more pronounced at high experimental temperatures.

It can be concluded that it is necessary to obtain pure ceramics to avoid transport losses, as well as the desire to reduce the temperature of heat treatment of the electrolyte layer to reduce the cost of production. Researchers have successfully developed ways to mitigate the sintering conditions of the electrolyte by modifying the synthesis methods, compaction of the layer and the introduction of a small amount of sintering aids, which together make it possible to obtain high-density ceramics at temperatures 150−300 °C lower than the initial 1500 °C. There are some papers that discuss the problems of the influence of synthesis routes on the reduction of the sintering temperature of LSGM electrolyte and microstructural and compositional effects related to its electrical and mechanical properties [35, 36]. The present review paper will be focused on obtaining pure ceramics using different fabrication techniques, different ways of densification of ceramic powder and the influence of sintering additives on the densification of the electrolyte layer.

2. Strategies for the reduction of the sintering temperature

The traditional solid state method can be used to prepare pure $La_{1-x}Sr_xGa_{1-y}Mg_yO_{3-\delta}$ ceramics at temperatures as high as 1450−1500 °C [17, 37]. Li et al. [11] were able to reduce the synthesis temperature of pure ceramics to 1400 °C by the solid state method, but for this they had to resort to a long 24-hour grinding of reagents at all intermediate stages of synthesis. The conductivity of the $La_{0.9}Sr_{0.1}Ga_{0.8}Mg_{0.2}O_{3-\delta}$ ceramic reaches 0.04−0.08 S/cm at 800 °C. From a production perspective, these approaches are considered expensive and need to be improved. In this section, various ceramic powder preparation methods are discussed to produce single phase materials with reduced heat treatment.

The different methods of LSGM electrolyte synthesis with the final preparation temperature of the ceramics are summarized in Table 2. The glycine-nitrate method can be used to produce single phase powders at temperatures of 1350−1400 °C. Nitrate salts are used as precursors with the addition of glycine as a fuel. The solution is heated in chemical beakers on a hotplate with slow evaporation and the formation of precursors with further self-ignition and formation of fine ash [25]. Samples crystallize into a cubic perovskite structure without the formation of any secondary phases [38]. Under conditions of rapid heating at 80−92 °C, secondary phases $LaSrGaO_4$ and $LaSrGa_3O_7$ crystallize at

the grain boundary of LSGM, which are stable even after heat treatment at 1400 °C. The single phase material is obtained by slow heating and evaporation at 92 °C. The pure material is described by a cubic structure with the $Pm\text{-}3m$ space group, in the presence of impurity phases the structure of $La_{0.9}Sr_{0.1}Ga_{0.8}Mg_{0.2}O_{3-\delta}$ is described by an orthorhombic structure (the space group $Imma$) [34]. The total conductivity of the samples synthesized by the glycine-nitrate method varies from 0.04−0.09 S/cm at 800 °C with different crystal structure and impurity concentration.

The freeze-drying method allows obtaining single-phase materials from oxide reagents that are dissolved in nitric acid [39, 51]. The mixture of reagents was pre-synthesized at 1200 °C because gallium oxide is insoluble in nitric acid, whereas the intermediates are soluble in acidic solution at 1200 °C. Ethylenediaminetetraacetic acid (EDTA) is introduced as a complexing agent followed by the addition of ammonia. These solutions are frozen in liquid nitrogen and then dehydrated in a freeze dryer. A stepwise heat treatment is then used to remove the organics, synthesize the powder, and produce the ceramics. Using this technology, pure $La_{1-x}Sr_xGa_{0.8}Mg_{0.2}O_{3-\delta}$ can be obtained at temperatures of 1350−1400 °C, depending on the strontium content in the composition. The structure of $La_{1-x}Sr_xGa_{0.8}Mg_{0.2}O_{3-\delta}$ solid solution changes with increasing strontium incorporation from orthorhombic ($Imma$) for $x = 0.1$ to cubic ($Pm\text{-}3m$) for $x = 0.2$. The total conductivity of the $La_{1-x}Sr_xGa_{0.8}Mg_{0.2}O_{3-\delta}$ ceramics is strongly dependent on the final heat treatment temperature (1300−1500 °C) and can vary from 0.08 to 0.11 S/cm.

Carbonate and hydroxycarbonate co-precipitation methods do not allow achieving high purity of lanthanum gallate [27, 40]. The formation of a phase mixture occurs with the presence of $LaSrGaO_4$ and $LaSrGa_3O_7$ oxides. A density of 93 % can be obtained using ammonium carbonate, and the conductivity of the ceramics does not exceed 0.045 S/cm.

The ethylene-glycol method produces ceramics of high purity and density (more than 99 %) with a particle size after synthesis of about 120 nm and a grain size of 6−8 μm at a sintering temperature of 1400 °C [41, 52]. The total conductivity of the LSGM ceramics is 0.056 S/cm at 800 °C. The synthesis method consists of sequentially dissolving the starting components in nitric acid, followed by the addition of ethylene glycol and urea. The reaction mixture is heated to 150 °C with a reflux condenser until precipitation is complete.

Hydrolysis of urea (NH_2CONH_2) produces NH_4OH, which acts as a precipitator of La^{3+}, Sr^{2+}, Ga^{3+}, and Mg^{2+}

Table 2 – Methods, synthesis conditions and impurities for Sr/Mg doped lanthanum gallate.

Synthesis method	Material	Pre-synthesis conditions	Additional phases	Compacting conditions	Impurity	Density	Ref
solid state	$La_{0.9}Sr_{0.1}Ga_{0.8}Mg_{0.2}O_{3-\delta}$	1250 °C, 20 h	$LaSrGaO_4$	1400 °C, 4 h	no	98 %	[11]
solid state	$La_{0.9}Sr_{0.1}Ga_{0.8}Mg_{0.2}O_{3-\delta}$	1250 °C, 24 h	–	1500 °C, 36 h	no	95 %	[17]
glycine-nitrate	$La_{0.9}Sr_{0.1}Ga_{0.8}Mg_{0.2}O_{3-\delta}$	1000 °C, 10 h	–	1350 °C, 10 h	no	95 %	[38]
glycine-nitrate	$La_{0.9}Sr_{0.1}Ga_{0.8}Mg_{0.2}O_{3-\delta}$	80 °C; 700 °C, 1 h	–	1400 °C, 6 h	no	99 %	[34]
freeze-drying	$La_{0.9}Sr_{0.1}Ga_{0.8}Mg_{0.2}O_{3-\delta}$	1200 °C, 4 h; 1250 °C, 4 h	$LaSrGaO_4$, $LaSrGa_3O_7$	1300 °C, 4 h	no	99 %	[39]
freeze-drying	$La_{0.8}Sr_{0.2}Ga_{0.8}Mg_{0.2}O_{3-\delta}$	1300 °C, 4 h; 1350 °C, 4 h	$LaSrGaO_4$, $LaSrGa_3O_7$	1400 °C, 20 min	no	100 %	[39]
carbonates co-precipitation	$La_{0.9}Sr_{0.1}Ga_{0.8}Mg_{0.2}O_{3-\delta}$	1100 °C, 6 h	$LaSrGaO_4$, $LaSrGa_3O_7$	1400 °C, 6 h	$LaSrGaO_4$, $LaSrGa_3O_7$	93 %	[40]
carbonates and hydroxyl-carbonates co-precipitation	$La_{0.8}Sr_{0.2}Ga_{0.8}Mg_{0.2}O_{3-\delta}$	1000 °C, 10 h	$LaSrGa_3O_7$, $LaSrGaO_4$, $La_4Ga_2O_9$	1400 °C, 10 h	$LaSrGa_3O_7$, $LaSrGaO_4$	93 %	[27]
ethylene glycol	$La_{0.9}Sr_{0.1}Ga_{0.8}Mg_{0.2}O_{3-\delta}$	1100 °C, 12 h	$LaSrGa_3O_7$, $LaSrGaO_4$, $La_4Ga_2O_9$	1400 °C, 6 h	no	99 %	[41]
acetate sol-gel	$La_{0.8}Sr_{0.2}Ga_{0.83}Mg_{0.17}O_{3-\delta}$	150 °C, 8 h; 300 °C, 2 h; 500 °C, 2 h; 700 °C, 2 h	La_2O_3, $LaSrGa_3O_7$, $La_2O_2CO_3$	1400 °C, 4 h	no	94 %	[42]
citrate sol-gel	$La_{0.9}Sr_{0.1}Ga_{0.8}Mg_{0.2}O_{3-\delta}$	800 °C	$LaSrGa_3O_7$, $LaSrGaO_4$	1400 °C, 9 h	$LaSrGa_3O_7$	–	[43]
regenerative sol-gel	$La_{0.8}Sr_{0.2}Ga_{0.85}Mg_{0.15}O_{3-\delta}$	900 °C, 6 h	$LaSrGaO_4$, $LaSrGa_3O_7$	1400 °C, 8 h	no	89 %	[44]
polymeric-gel	$La_{0.8}Sr_{0.2}Ga_{0.83}Mg_{0.17}O_{3-\delta}$	1000 °C, 6 h	$La_4Ga_2O_9$, $LaSrGa_3O_7$, $LaSrGaO_4$	1450 °C, 10 h	no	97 %	[33]
ultrasonic spray pyrolysis	$La_{0.9}Sr_{0.1}Ga_{0.8}Mg_{0.2}O_{3-\delta}$	1000 °C, 6 h	$La_4Ga_2O_9$, $LaSrGaO_4$, $Sr_3Ga_2O_6$	1500 °C, 6 h	no	96 %	[45]
acrylamide polymerization	$La_{0.85}Sr_{0.15}Ga_{0.85}Mg_{0.15}O_{3-\delta}$	1000 °C, 6 h; 1200 °C, 6 h; 1300 °C, 6 h	$La_4Ga_2O_9$, $LaSrGaO_4$, $LaSrGa_3O_7$, $Sr_3Ga_2O_6$	1500 °C, 15 h	$LaSrGa_3O_7$	98 %	[46]
self-propagating high-temperature	$La_{0.9}Sr_{0.1}Ga_{0.8}Mg_{0.2}O_{3-\delta}$	1000 °C, 6 h	La_2O_3, Ga_2O_3, $LaSrGa_3O_7$	1400 °C, 9 h	no	98 %	[47]
microwave-induced	$La_{0.8}Sr_{0.2}Ga_{0.83}Mg_{0.17}O_{3-\delta}$	900 °C, 6 h	$LaSrGaO_4$, $LaSrGa_3O_7$	1400 °C, 9 h	no	–	[48]
hydrothermal urea precipitation	$La_{0.8}Sr_{0.2}Ga_{0.8}Mg_{0.2}O_{3-\delta}$	800 °C, 12 h	$GaO(OH)$, $La(OH)_3$, La_2O_3	900 °C, 12 h	no	98 %	[49]
laser rapid solidification	$La_{0.8}Sr_{0.2}Ga_{0.83}Mg_{0.17}O_{3-\delta}$	100 °C, 2 h	–	1100 W CO_2 laser power, 1 mm/s scan speed	no	97 %	[50]

ions to form the corresponding oxides and/or hydroxides.

One of the most common methods for the synthesis of ceramic materials is the sol-gel method, which has various modifications depending on the type of complexing agent and initial reagents [33, 42–44, 53].

The general approach to synthesis is to dissolve initial reagents with addition of complexing agent and slow evaporation of the solution to obtain a gel-like mass. Further steps are performed stepwise for the sequential decomposition of complexes and the formation of the main fine phase of the substance, and with intermediate

grinding of the precursor. In most cases, this synthesis method leads to the formation of single-phase finely dispersed LSGM powder with cubic structure at synthesis temperatures of 1400−1450 °C. The conductivity of the ceramics varies in the range of 0.051−0.082 S/cm at 800 °C and depends on the grain size. The grain size strongly affects the grain boundary resistivity compared to the bulk resistivity, but no significant difference is observed in the total conductivity.

The ultrasonic spray pyrolysis technique is based on the thermal decomposition of nitrate salt aerosol in a tube furnace at 900 °C, obtained by ultra-high-frequency spraying of an aqueous precursor solution [45]. The resulting powder was partially crystallized and is a mixture of $La_{0.9}Sr_{0.1}Ga_{0.8}Mg_{0.2}O_{3-\delta}$ and $La_4Ga_2O_9$ and La_4SrO_7, indicating that the reaction is incomplete. The final synthesis was carried out at 1500 °C with holding times ranging from 6 to 48 hours, which is comparable to the solid state method.

The acrylamide polymerization method is ideologically similar to the sol-gel method [46]. EDTA $[CH_2N(CH_2COOH)_2]_2$ is used as a complexing agent with the addition of NH_4OH to generate chelating cations, followed by the addition of acrylamide monomers $CH_2CHCONH_2$ to form polyacrylamide chains and the crosslinking agent N,N'-methylene-bis-acrylamide to achieve the final topology of the gel complex. The synthesized powders consist of micron-sized thin plates aggregated by a large number of ultrafine particles. However, it is not possible to obtain a single phase material even at 1500 °C for 15 hours. The composition identifies the presence of $LaSrGa_3O_7$ phase with a relative material density of 97.6 %, and the total conductivity of the ceramic is 0.093 S/cm at 800 °C.

Application of self-propagating high-temperature synthesis allows obtaining finely dispersed powders with an average particle size of 1.6 μm [47]. The peculiarity of the synthesis is the reaction combustion of the compacted initial reagents in a closed graphite crucible in an argon atmosphere. An igniter made of disposable carbon foil, placed in contact with one end of the sample, was subjected to electrical ignition at a voltage of 50 V and a current of 100 A at room temperature. The resulting sample was poured into water and washed with an ultrasonic cleaner to remove salts from the final product. Ceramics with a density of 98 % were formed at a lower sintering temperature of 1400 °C compared to the solid state method. The electrical conductivity of $La_{0.9}Sr_{0.1}Ga_{0.8}Mg_{0.2}O_{3-\delta}$ electrolyte reaches 0.11 S/cm at 800 °C, which is attractive for practical use as an electrolyte for SOFCs in the mid-temperature operating range.

The method of polymerization of polyvinyl alcohol solution for the synthesis of LSGM electrolyte induced by microwave irradiation is performed in a modified microwave oven furnace [48]. Small, homogeneous and high-density $La_{0.8}Sr_{0.2}Ga_{0.83}Mg_{0.17}O_{3-\delta}$ electrolyte particles with an average size of 2−3 μm can be observed after heat treatment at 1400 °C for 9 hours. The homogeneous mixing method and the steric entrapment mechanism by the large chain molecules of the polyvinyl alcohol lead to a stoichiometric and homogeneous powder.

The pure $La_{0.8}Sr_{0.2}Ga_{0.8}Mg_{0.2}O_{3-\delta}$ powder can be obtained at 900 °C by the hydrothermal urea hydrolysis precipitation technique with a particle size of about 150 nm [49]. However, a dense 98 % ceramic from the powder can only be obtained at 1400 °C for 3 h of exposure time. The conductivity of the sample obtained by hydrothermal urea hydrolysis is 0.056 S/cm at 800 °C, which is comparable in value to the ceramics obtained by sol-gel methods.

The rapid laser solidification method allows obtaining of single-phase materials without high-temperature heat treatment [50]. Samples obtained by this method form unique lance-shaped or sheet-like microstructures that are ordered and densely packed. The essence of the method is the melting of a compact precursor under the action of a CO_2 laser with a power of 1100 W and a scan rate of 1 mm/s. The $La_{0.8}Sr_{0.2}Ga_{0.83}Mg_{0.17}O_{3-\delta}$ powder is produced as a single-phase powder crystallized in an orthorhombic structure. The density of the ceramics is 97.2 % of the theoretical density, and the total conductivity is 0.09 S/cm at 800 °C.

The use of solution synthesis methods leads to the formation of finely dispersed powders, which improves sintering into a dense substrate and increases the extent of contacts between grains. Rambabu et al. [44] presented the dependencies of total conductivity, bulk and grain boundary resistances for $La_{0.8}Sr_{0.2}Ga_{0.83}Mg_{0.17}O_{3-\delta}$ ceramics sintered at temperatures of 1400−1500 °C. It is shown that there is no significant difference in the total conductivity. The bulk resistivity is very close to each other, but its grain boundary resistivity decreases by a factor of 2.7 with increasing grain size from 3.5 μm to 10 μm. Similar trends in grain boundary resistance variation with grain size of LSGM ceramics have been reported in other papers [38, 54, 55]. Chen et al. [55] suggest an increasing grain boundary space charge effect with increasing sintering temperature/grain size, which is consistent with increasing compositional uniformity by TEM.
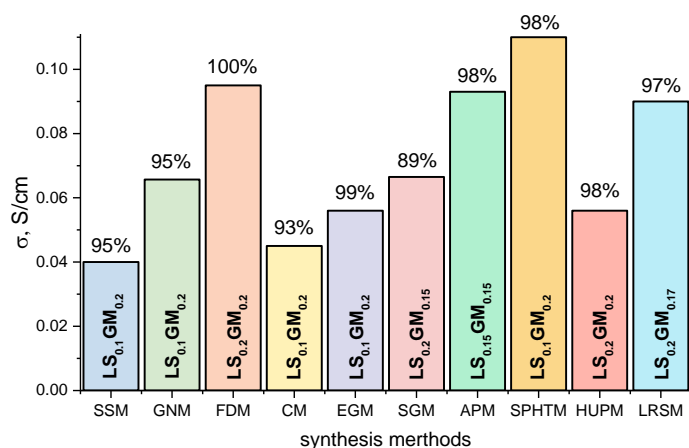
Figure 1 Conductivity of LSGM samples at 800 °C prepared by different methods: SSM – solid state [17]; GNM – glycine-nitrate [38]; FDM – freeze-drying [39]; CM – carbonate [40]; EGM – ethylene glycol [41]; SGM – sol-gel [44]; APM–acrylamide polymerization [46]; SPHTM – self-propagating high-temperature [47]; HUPM – hydrothermal urea precipitation [49]; LRSM – laser rapid solidification [50]. Density of material is given in %.

STEM−EDS mapping revealed distinct regions of cationic heterogeneity at grain boundaries: Sr-rich phases and Mg-rich nanoscale regions. Apparently, their minor presence does not affect the general trend of grain boundary conductivity enhancement.

According to the results, it can be concluded that solution synthesis methods or other modified approaches lead to the production of single-phase powdered LSGM electrolyte at temperatures lower than the traditional solid state method. However, to obtain dense ceramics, high-temperature heat treatment of compact materials is often required, in which case the fabrication temperature is 1400−1500 °C. The total conductivity of materials fabricated by solution methods is equal or higher with the traditional fabrication approach, Figure 1.

Further developments to minimize power costs of ceramics production involve modifying or changing the technological approaches to create a dense ceramic layer through the application/deposition of films and using sintering aids. The following sections describe these developments.

3. Influence of formation methods and sintering additives on the properties of ceramics

Isostatic pressing of a green material prior to high pressure sintering is considered as one of the ways to increase the electrolyte density [17, 56–58]. The main advantage of isostatic treatment is the homogeneity of the density distribution over the volume of the part, which further influences the shrinkage of the material during sintering. The bar formed under the pressure of

200 MPa for 10 min results in a 50−100 °C decrease in heat treatment temperature, and the density of the material is about 96 % of the theoretical [17]. Using hot isostatic pressing, porous LSGM with a relative density of 99.6 % was obtained at 1300 °C for 1 h under the pressure of 200 MPa, which is 200 °C lower than the solid state method [57].

Dense coatings of 20−60 µm thick LSGM can be obtained by atmospheric plasma spraying [54, 59–62]. In this coating method, the material to be sprayed is heated to a liquid state and transferred to the surface to be treated by means of a plasma steam. The temperature was equal to or higher than the melting point (1723 °C) of the LSGM material. To achieve the liquid state of the material, different arc powers were experimentally selected depending on the particle size of the dispersed powder. Large uniform grains within the coatings indicate epitaxial growth of interlayer boundaries and improved coating quality. With increasing particle temperature, the conductivity of dense LSGM coatings deposited by atmospheric plasma spraying is comparable to that of bulk material and the cell performance is significantly improved. LSGM material can be sintered to a fully dense state by current-limited flash sintering method at a temperature of 690 °C in an electric field of 60−120 V/cm [63]. The exposure time does not exceed 10 minutes, which can significantly simplify the production of ceramics.

The centrifugal casting method produces high density multilayer electrolyte layers [64–66]. The thickness of the layers can be controlled by the amount and density of the slurry. The sintering temperature to obtain a dense layer varies in the range of 900−1400 °C depending on the microstructural characteristics of the LSGM powder and slurry. A cold vacuum spraying method with a two-layer design can be used to seal LSGM coatings [67]. Nano-structured LSGM coatings with a thickness of ~5 µm are formed after low-temperature sintering at 1200 °C [68]. An electrolyte slab with a thickness of about 180 µm can be obtained by the tape casting method. The process uses powder slurry containing ethanol and toluene and organic additives, which is spread evenly over the surface of the substrate with a doctor blade. The heat treatment reaches 1460 °C at which the relative density of the material is 96 %.

Another technological method to increase the density of the material at reduced temperatures is the introduction of sintering aids. Small amounts of additives are introduced in the form of nitrates or oxides. The nature of the alloying metal and the concentration of the additive determine the ceramic grain size, phase stability, material density, total conductivity, and grain boundary

Figure 2 Sintering aids and their influence on ceramic properties.

resistance. Ha et al. [69] investigated a series of 1 % additives introduced via metal nitrates into $La_{0.8}Sr_{0.2}Ga_{0.8}Mg_{0.2}O_{3-\delta}$ powder. The best results for ceramic densification at 1300 °C were achieved by the addition of V^{5+}, Li^+, and Cu^{2+} ions, for phase purity by the addition of B^{3+}, V^{5+}, and Si^{4+}, and for electrical conductivity by the addition of V^{5+}, Fe^{3+}, Zn^{2+}, and Cu^{2+}. For Si^{4+} in ceramics, a decrease in total resistivity is observed due to a decrease in grain boundary resistivity. The introduction of V^{5+}, Fe^{3+}, Al^{3+}, Co^{2+}, Ni^{2+}, Zn^{2+}, Mn^{4+}, and Ca^{2+} ions decreases the grain boundary resistivity and the total resistance of ceramics, which can be explained by the presence of sintering additives at the grain boundaries and partial introduction of sintering agents of additives into the lattice of LSGM. The addition of Ba^{2+} decreases the phase purity during sintering at 1300 °C and increases the total resistance of the material. The interdiffusion between NiO and LSGM electrolyte is described in [70]. The concentration of nickel oxide at the grain boundary decreases from 2 % to 0.5 %, resulting in the formation of $LaSrGa(Ni)O_4$-type phase. The presence of nickel leads to an increase in the conductivity of the ceramics in air due to the formation of hole conductivity, and it decreases significantly under conditions of reduced oxygen pressure due to the formation of $LaSrGa(Ni)O_4$-type phase.

In [71], it was observed that the addition of V_2O_5 promotes the densification and purity of the phase, which is attributed to the improvement of sintering and mass transfer by liquid phase sintering. $La_{0.8}Sr_{0.2}Ga_{0.8}Mg_{0.2}O_{3-\delta} + 1\%VO_{5/2}$ ceramics exhibit a high ionic conductivity of ~0.027 S/cm at 700 °C. In contrast, Larregle et al. [72] showed that the addition of V_2O_5 resulted in the worst performance in terms of compaction and phase purity, leading to the formation of unknown phases, probably caused by a reactive process favored by the high density of grain boundaries.

The addition of 1 % Li_2O sintering aid to the $La_{0.8}Sr_{0.2}Ga_{0.8}Mg_{0.2}O_{3-\delta}$ electrolyte promotes the preparation of 99 % dense ceramics at 1400 °C [73]. The additive eliminates the impurity phase of $LaSrGa_3O_7$ in LSGM ceramics, suppresses the formation of the impurity phase of MgO, and increases the ionic conductivity by 20 % to a value of 0.17 S/cm at 800 °C.

The introduction of bismuth oxide in the amount of 1.2 % to 4.8 % into $La_{0.9}Sr_{0.1}Ga_{0.8}Mg_{0.2}O_{3-\delta}$ has a positive effect on the sintering process [74]. The compaction temperature does not exceed 1300 °C, but pores remain in the ceramic even when 4.8 % Bi_2O_3 is introduced. Regardless of the concentration of the bismuth oxide additive, its presence has a negative effect on the ionic conductivity. The ionic conductivity of $La_{0.9}Sr_{0.1}Ga_{0.8}Mg_{0.2}O_{3-\delta} + 1.2\% Bi_2O_3$ decreases from $2 \cdot 10^{-3}$ to $3 \cdot 10^{-4}$ S/cm in the temperature range of 500–700 °C, apparently due to the chemical interaction of the components.

Larregle et al. [72] showed that the addition of 2 % ZnO or Fe_2O_3 leads to its incorporation into the LSGM lattice, which allows to obtain dense electrolytes at 1350 °C. In $La_{0.8}Sr_{0.2}Ga_{0.8}Mg_{0.2}O_{3-\delta} + 2\% Fe_2O_3$ ceramics, a nonlinear dependence of grain boundary conductivity is observed, which is probably due to two

factors with increasing time during sintering of the material, namely grain size increase and strontium segregation with phase formation at the boundary.

By adding 0.5–1.5 % Ga_2O_3 into $La_{0.9}Sr_{0.1}Ga_{0.8}Mg_{0.2}O_{3-\delta}$, ceramic with 95 % relative density at 1350 °C can be achieved [75]. This addition enhances grain growth from 2.3 to 3.2 μm, confirming the inclusion of $La_4Ga_2O_9$, $LaSrGa_3O_7$, and $LaSrGaO_4$ in the electrolyte structure and the formation of new phases at the grain boundary. The addition of 1.0 mol % of Ga_2O_3 to the material yields favorable results, showing an increase in bulk conductivity of ~22 % and an increase in grain boundary conductivity of ~35 % at a temperature of 320 °C.

Molybdenum oxide is an effective sintering aid that optimizes the electrical properties of LSGM electrolyte [76]. By introducing 1.23 % MoO_3, the density and grain size increase, while the bulk resistivity decreases by a factor of 1.12 and along grain boundaries by a factor of 1.73 at 500 °C. In the MoO_3 doped LSGM, some MoO_3 is introduced into the electrolyte structure and distributed along the grain boundaries [77]. The sintering aid partially volatilizes at 1300 °C.

Thus, the literature suggests ways to improve the efficiency of obtaining a compact ceramic substrate or membrane by changing the deposition technology and introducing different sintering additives. The electrochemical properties of the electrolyte are not positively affected by all of the sintering additives. These characteristics are summarized in Figure 2.

4. Conclusions

Literature studies show that it is critical to produce LSGM ceramics at lower temperatures. This can be achieved by modifying synthesis methods, adding sintering additives, and compacting the powder or depositing it on a substrate. Lowering the sintering temperature has a positive impact on optimizing the production conditions of electrochemical cells and reducing energy costs, which ultimately lowers the overall cost. Control is necessary when selecting a synthesis method and sintering additive, as not all methods produce single-phase LSGM ceramics and some additives reduce the purity and ionic conductivity of the electrolyte. Solution synthesis methods have proven to be most effective in achieving a single-phase composition at lower temperatures. Metal oxides, such as Fe_2O_3, Al_2O_3, CoO, NiO, and Mn_2O_3, can serve as promising sintering aids due to their ability to increase density, improve ionic conductivity, and enhance phase stability of materials. Conducting thorough research and development in this area is highly conducive to the production of an effective electrolyte layer in electrochemical devices.

Supplementary materials

No supplementary materials are available.

Funding

Acknowledgments

Author contributions

Egor Gordeev: Data curation; Formal Analysis; Writing – Original draft.

Natalia Porotnikova: Conceptualization; Writing – Original draft; Writing – Review & Editing.

Conflict of interest

The authors declare no conflict of interest.

Additional information

Egor Gordeev, Author ID: 57204039544; Orcid: 0000-0001-7822-9049.

Natalia Porotnikova, Author ID: 36508916000; Orcid: 0000-0001-5284-4553; Web of Science ResearcherID: J-7625-2016.

References

1. Jiao K, Xuan J, Du Q, Bao Zh, et al., Designing the next generation of proton-exchange membrane fuel cells, Nature, **595** (2021) 361–369. https://doi.org/10.1038/s41586-021-03482-7

2. Develos-Bagarinao K, Ishiyama T, Kishimoto H, Shimada H, et al., Nanoengineering of cathode layers for solid oxide fuel cells to achieve superior power densities, Nat. Commun., **12** (2021) 3979. https://doi.org/10.1038/s41467-021-24255-w

3. Xu Q, Guo Z, Xia L, He Q, et al., A comprehensive review of solid oxide fuel cells operating on various promising alternative fuels. Energy Convers. Manag., **253** (2022) 115175. https://doi.org/10.1016/j.enconman.2021.115175

4. Ananchenko DV, Nikiforov SV, Sobyanin KV, Konev SF, et al., Paramagnetic Defects and Thermoluminescence in Irradiated Nanostructured Monoclinic Zirconium Dioxide, Materials, **15** (2022) 8624. https://doi.org/10.3390/ma15238624

5. Erpalov MV, Tarutin AP, Danilov NA, Osinkin DA, et al., Chemistry and electrochemistry of CeO_2-based interlayers: Prolonging the lifetime of solid oxide fuel and electrolysis cells, Russ. Chem. Rev., **92** (2023) RCR5097. https://doi.org/10.59761/RCR5097

6. Politov BV, Antonova EP, Tropin ES, Osinkin DA, et al., Highly efficient all-perovskite fuel cell for intermediate temperature range, Renew. Energy, **206** (2023) 872–878. https://doi.org/10.1016/j.renene.2023.02.070

7. Gordeev E, Belyakov S, Antonova E, Osinkin D, Highly Conductive Fe-Doped $(La,Sr)(Ga,Mg)O_{3-\delta}$ Solid-State Membranes for Electrochemical Application, Membranes, **13** (2023) 502. https://doi.org/10.3390/membranes13050502

8. Kharton VV, Shaula AL, Vyshatko NP, Marques FMB, Electron-hole transport in $(La_{0.9}Sr_{0.1})_{0.98}Ga_{0.8}Mg_{0.2}O_{3-\delta}$ electrolyte: effects of ceramic microstructure, Electrochimica Acta, **48** (2003) 1817–1828. https://doi.org/10.1016/S0013-4686(03)00247-0

9. Stevenson J, Effect of A-site cation nonstoichiometry on the properties of doped lanthanum gallate, Solid State Ion., **113–115** (1998) 571–583. https://doi.org/10.1016/S0167-2738(98)00324-5

10. Huang K, Tichy RS, Goodenough JB, Superior Perovskite Oxide-Ion Conductor; Strontium- and Magnesium-Doped $LaGaO_3$: I, Phase Relationships and Electrical Properties, J. Am. Ceram. Soc., **81** (2005) 2565–2575. https://doi.org/10.1111/j.1151-2916.1998.tb02662.x

11. Li M, Zhang Y, An M, Lu Zh, et al., Synthesis and characterization of $La_{0.9}Sr_{0.1}Ga_{0.8}Mg_{0.2}O_{3-\delta}$ intermediate-temperature electrolyte using conventional solid state reaction, J. Power Sources, **218** (2012) 233–236. https://doi.org/10.1016/j.jpowsour.2012.06.101

12. Huang K, Feng M, Goodenough JB, Sol-Gel Synthesis of a New Oxide-Ion Conductor Sr- and Mg-Doped $LaGaO_3$ Perovskite, J. Am. Ceram. Soc., **79** (1996) 1100–1104. https://doi.org/10.1111/j.1151-2916.1996.tb08554.x

13. Kim J, Partial electronic conductivity and electrolytic domain of $La_{0.9}Sr_{0.1}Ga_{0.8}Mg_{0.2}O_{3-\delta}$, Solid State Ion., **140** (2001) 105–113. https://doi.org/10.1016/S0167-2738(01)00687-7

14. Vdovin GK, Kurumchin EKh, Isaeva EV, Bronin DI Isotopic Exchange and Oxygen Diffusion in the $La_{0.88}Sr_{0.12}Ga_{0.82}Mg_{0.18}O_{3-\alpha}$–Molecular Oxygen System, Russ. J. Electrochem., **37** (2001) 304–307. https://doi.org/10.1023/A:1009085532471

15. Kurumchin EKh, Ananjev MV, Vdovin GK, Surkova MG, Exchange kinetics and diffusion of oxygen in systems based on lanthanum gallate, Russ. J. Electrochem., **46** (2010) 205–211. https://doi.org/10.1134/S1023193510020126

16. Pandey R, Singh RK, Singh P, Synthesis of $La_{0.9}Sr_{0.1}Ga_{0.8}Mg_{0.2}O_{3-\delta}$ electrolyte via ethylene glycol route and its characterizations for IT-SOFC, Ceram. Int., **40** (2014) 7177–7184. https://doi.org/10.1016/j.ceramint.2013.12.056

17. Naiqing Z, Kening S, Derui Z, Dechang J, Study on Properties of LSGM Electrolyte Made by Tape Casting Method and Applications in SOFC, J. Rare Earths, **24** (2006) 90–92. https://doi.org/10.1016/S1002-0721(07)60331-7

18. Hayashi H, Saitou T, Maruyama N, Inaba H, et al., Thermal expansion coefficient of yttria stabilized zirconia for various yttria contents, Solid State Ion., **176** (2005) 613–619. https://doi.org/10.1016/j.ssi.2004.08.021

19. Lyagaeva J, Medvedev D, Pikalova E, Plaksin S, et al., A detailed analysis of thermal and chemical compatibility of cathode materials suitable for $BaCe_{0.8}Y_{0.2}O_{3-\delta}$ and $BaZr_{0.8}Y_{0.2}O_{3-\delta}$ proton electrolytes for solid oxide fuel cell application, Int. J. Hydrog. Energy, **42** (2017) 1715–1723. https://doi.org/10.1016/j.ijhydene.2016.07.248

20. Pikalova EYu, Kolchugin AA, The Influence of the Substituting Element (M = Ca, Sr, Ba) in $La_{1.7}M_{0.3}NiO_{4+\delta}$ on the Electrochemical Performance of the Composite Electrodes, Eurasian Chem-Technol. J., **18** (2016) 3. https://doi.org/10.18321/ectj386

21. Tietz F, Thermal expansion of SOFC materials. Ionics **5** (1999) 129–139. https://doi.org/10.1007/BF02375916

22. Yamamoto O, Solid oxide fuel cells: fundamental aspects and prospects, Electrochimica Acta, **45** (2000) 2423–2435. https://doi.org/10.1016/S0013-4686(00)00330-3

23. Liu Y, Qin H, Li M, Cheng J, et al., Direct synthesis of $Ce_{0.8}Sm_{0.2-x}Zn_xO_{2-\delta}$ electrolyte by sol–gel for IT-SOFC, Ionics, **28** (2022) 4675–4684. https://doi.org/10.1007/s11581-022-04677-2

24. Steele BCH, Heinzel A, Materials for fuel-cell technologies, Nature, **414** (2001) 345–352. https://doi.org/10.1038/35104620

25. Zheng F, Bordia RK, Pederson LR, Phase constitution in Sr and Mg doped $LaGaO_3$ system, Mater. Res. Bull., **39** (2004) 141–155. https://doi.org/10.1016/S0025-5408(03)00140-5

26. Tsipis EV, Waerenborgh JC, Kharton VV, Grain-boundary states in solid oxide electrolyte ceramics processed using iron oxide sintering aids: a Mössbauer spectroscopy study, J. Solid State Electrochem., **21** (2017) 2965–2974. https://doi.org/10.1007/s10008-017-3622-3

27. Cristiani C, Zampori L, Latorrata S, Pelosato R, et al., Carbonate coprecipitation synthesis of Sr- and Mg-doped $LaGaO_3$, Mater. Lett., **63** (2009) 1892–1894. https://doi.org/10.1016/j.matlet.2009.06.007

28. Rozumek M, Majewski P, Schluckwerder H, Aldinger F, et al., Electrical Conduction Behavior of $La_{1+x}Sr_{1-x}Ga_3O_{7-\delta}$ Melilite-Type Ceramics, J. Am. Ceram. Soc., **87** (2004) 1795–1798. https://doi.org/10.1111/j.1551-2916.2004.01795.x

29. Kuang X, Green MA, Niu H, Zajdel P, et al., Interstitial oxide ion conductivity in the layered tetrahedral network melilite structure, Nat. Mater., **7** (2008) 498–504. https://doi.org/10.1038/nmat2201

30. Kitamura N, Hamao N, Vogel SC, Idemoto Y, Oxide-Ion Conduction, Average and Local Structures of $LaSrGa_{1-x}Mg_xO_{4-\delta}$ with Layered Perovskite Structure, Electrochemistry, **81** (2013) 448–453. https://doi.org/10.5796/electrochemistry.81.448

31. Kosuge T, Kitamura N, Idemoto Y, Electrical Conduction Property and Crystal Structure of $Pr_{1+x}Sr_{1-x}GaO_{4+\delta}$, $Pr_{1+x}Sr_{1-x}Ga_3O_{7+\delta}$, ECS Meet. Abstr., **MA2010-02** (2010) 17–17. https://doi.org/10.1149/MA2010-02/1/17

32. Rozumek M, Majewski P, Aldinger F, Kunstler K, et al., Preparation and electrical conductivity of common impurity phases in $(La,Sr)(Ga,Mg)O_3$ solid electrolytes, (2003) CFI (Ceramic Forum International/Berichte der DKG)

33. Li T-W, Yang S-Q, Li S, Preparation and characterisation of perovskite $La_{0.8}Sr_{0.2}Ga_{0.83}Mg_{0.17}O_{2.815}$ electrolyte using a poly(vinylalcohol) polymeric method, J. Adv. Ceram., **5** (2016) 167–175. https://doi.org/10.1007/s40145-016-0186-0

34. Zhang Q, Liu WJ, Wang J, Liu D, et al., Processing of perovskite $La_{0.9}Sr_{0.1}Ga_{0.8}Mg_{0.2}O_{3-\delta}$ electrolyte by glycine-nitrate combustion method, Int. J. Hydrog. Energy, **46** (2021) 31362–31369. https://doi.org/10.1016/j.ijhydene.2021.07.003

35. Morales M, Roa JJ, Tartaj J, Segarra M, A review of doped lanthanum gallates as electrolytes for intermediate temperature solid oxides fuel cells: From materials processing to electrical and thermo-mechanical properties, J. Eur. Ceram. Soc., **36** (2016) 1–16. https://doi.org/10.1016/j.jeurceramsoc.2015.09.025

36. Filonova E, Medvedev D, Recent Progress in the Design, Characterisation and Application of $LaAlO_3$- and $LaGaO_3$-Based Solid Oxide Fuel Cell Electrolytes, Nanomaterials, **12** (2022) 1991. https://doi.org/10.3390/nano12121991

37. Seong Y-H, Jo S-H, Muralidharan P, Kim D-K, Synthesis and Characterization of LSGM Solid Electrolyte for Solid Oxide Fuel Cell, J. Korean. Ceram. Soc., **44** (2007) 696–702. https://doi.org/10.4191/KCERS.2007.44.1.696

38. Yu S, Bi H, Sun J, Zhu L, et al., Effect of grain size on the electrical properties of strontium and magnesium doped lanthanum gallate electrolytes, J. Alloys Compd., **777** (2019) 244–251. https://doi.org/10.1016/j.jallcom.2018.10.257

39. Marrero-López D, Ruiz-Morales JC, Peña-Martínez J, Martin-Sedeno MC, et al., Influence of phase segregation on the bulk and grain boundary conductivity of LSGM electrolytes, Solid State Ion., **186** (2011) 44–52. https://doi.org/10.1016/j.ssi.2011.01.015

40. Chae NS, Park KS, Yoon YS, Kim JS, et al., Sr- and Mg-doped $LaGaO_3$ powder synthesis by carbonate coprecipitation, Colloids Surf. Physicochem. Eng. Asp., 313–314 (2008) 154–157. https://doi.org/10.1016/j.colsurfa.2007.04.084

41. Raghvendra P, Kumar SR, Singh P, Synthesis of $La_{0.9}Sr_{0.1}Ga_{0.8}Mg_{0.2}O_{3-\delta}$ electrolyte via ethylene glycol route and its characterizations for IT-SOFC, Ceram. Int., **40** (2014) 7177–7184. https://doi.org/10.1016/j.ceramint.2013.12.056

42. Huang K, Goodenough JB, Wet Chemical Synthesis of Sr- and Mg-Doped $LaGaO_3$, a Perovskite-Type Oxide-Ion Conductor, J. Solid State Chem., **136** (1998) 274–283. https://doi.org/10.1006/jssc.1997.7706

43. Polini R, Pamio A, Traversa E, Effect of synthetic route on sintering behaviour, phase purity and conductivity of Sr- and Mg-doped $LaGaO_3$ perovskites, J. Eur. Ceram. Soc., **24** (2004) 1365–1370. https://doi.org/10.1016/S0955-2219(03)00592-2

44. Rambabu B, Ghosh S, Zhao W, Jena H, Innovative processing of dense LSGM electrolytes for IT-SOFC's, J. Power Sources, **159** (2006) 21–28. https://doi.org/10.1016/j.jpowsour.2006.04.107

45. Djurado E, Labeau M, Second phases in doped lanthanum gallate perovskites, J. Eur. Ceram. Soc., **18** (1998) 1397–1404. https://doi.org/10.1016/S0955-2219(98)00016-8

46. Liu N, Yuan Y, Majewski P, Aldinger F, Synthesis of $La_{0.85}Sr_{0.15}Ga_{0.85}Mg_{0.15}O_{2.85}$ materials for SOFC applications by acrylamide polymerization, Mater. Res. Bull., **41** (2006) 461–468. https://doi.org/10.1016/j.materresbull.2005.09.022

47. Ishikawa H, Enoki M, Ishihara T, Akiyama T, Self-propagating high-temperature synthesis of $La(Sr)Ga(Mg)O_{3-\delta}$ for electrolyte of solid oxide fuel cells, J. Alloys Compd., **430** (2007) 246–251. https://doi.org/10.1016/j.jallcom.2006.05.003

48. Zhai Y, Ye C, Xia F, Xiao J, et al., Preparation of $La_{0.8}Sr_{0.2}Ga_{0.83}Mg_{0.17}O_{2.815}$ powders by microwave-induced poly(vinylalcohol) solution polymerization, J. Power Sources, 162 (2006) 146–150. https://doi.org/10.1016/j.jpowsour.2006.06.069

49. Chen T-Y, Fung K-Z, Synthesis of and densification of oxygen-conducting $La_{0.8}Sr_{0.2}Ga_{0.8}Mg_{0.2}O_{2.8}$ nano powder prepared from a low temperature hydrothermal urea precipitation process, J. Eur. Ceram. Soc., **28** (2008) 803–810. https://doi.org/10.1016/j.jeurceramsoc.2007.08.006

50. Zhang J, Yuan C, Wang J-Q, Er-Jun L, et al., Oxygen ion conductivity of $La_{0.8}Sr_{0.2}Ga_{0.83}Mg_{0.17-x}Co_xO_{3-\delta}$ synthesized by laser rapid solidification, Chin. Phys. B, **22** (2013) 087201. https://doi.org/10.1088/1674-1056/22/8/087201

51. Marrero-López D, Martín-Sedeño MC, Peña-Martínez J, Ruiz-Morales JC, et al., Microstructure and Conductivity of $La_{1-x}Sr_xGa_{0.8}Mg_{0.2}O_{3-\delta}$ Electrolytes Prepared Using the Freeze-Drying Method: Microstructure and Conductivity of LSGM Electrolytes, J. Am. Ceram. Soc., **94** (2011) 1031–1039. https://doi.org/10.1111/j.1551-2916.2010.04233.x

52. Tas AC, Majewski PJ, Aldinger F, Chemical Preparation of Pure and Strontium- and/or Magnesium-Doped Lanthanum Gallate Powders. Chem. Inform., **32(12)** (2001) 1. https://doi.org/10.1002/chin.200112015

53. Wang XP, Zhou DF, Yang GC, Sun SC, et al., Nonstoichiometric $(La_{0.95}Sr_{0.05})_xGa_{0.9}Mg_{0.1}O_{3-\delta}$ electrolytes and $Ce_{0.8}Nd_{0.2}O_{1.9}-(La_{0.95}Sr_{0.05})_xGa_{0.9}Mg_{0.1}O_{3-\delta}$ composite electrolytes for solid oxide fuel cells, Int. J. Hydrog. Energy, **39** (2014) 1005–1013. https://doi.org/10.1016/j.ijhydene.2013.10.096

54. Wang Y-P, Gao J-T, Li J-H, Li Ch-J, et al., Preparation of bulk-like $La_{0.8}Sr_{0.2}Ga_{0.8}Mg_{0.2}O_{3-\delta}$ coatings for porous metal-supported solid oxide fuel cells via plasma spraying at increased particle temperatures, Int. J. Hydrog. Energy, **46** (2021) 32655–32664. https://doi.org/10.1016/j.ijhydene.2021.07.121

55. Chen T, Harrington GF, Matsuda J, Sasaki K, et al., Modifying Grain Boundary Ionic/Electronic Transport in Nano-Sr- and Mg- Doped $LaGaO_{3-\delta}$ by Sintering Variations, J. Electrochem. Soc., **166** (2019) F569–F580. https://doi.org/10.1149/2.0151910jes

56. Morales M, Pérez-Falcón JM, Moure A, Tartaj J, et al., Performance and degradation of $La_{0.8}Sr_{0.2}Ga_{0.85}Mg_{0.15}O_{3-\delta}$ electrolyte-supported cells in single-chamber configuration, Int. J. Hydrog. Energy, **39** (2014) 5451–5459. https://doi.org/10.1016/j.ijhydene.2014.01.019

57. Ohnuki M, Fujimoto K, Ito S, Preparation of high-density $La_{0.90}Sr_{0.10}Ga_{1-y}Mg_yO_{3-\delta}$ (y=0.20 and 0.30) oxide ionic conductors using HIP. Solid State Ion., **177** (2006) 1729–1732. https://doi.org/10.1016/j.ssi.2006.04.020

58. Morales M, Roa JJ, Tartaj J, Segarra M Performance and short-term stability of single-chamber solid oxide fuel cells based on $La_{0.9}Sr_{0.1}Ga_{0.8}Mg_{0.2}O_{3-\delta}$ electrolyte, J. Power Sources, **216** (2012) 417–424. https://doi.org/10.1016/j.jpowsour.2012.05.076

59. Zhang S-L, Liu T, Li C-J, Yao Sh-W, et al., Atmospheric plasma-sprayed $La_{0.8}Sr_{0.2}Ga_{0.8}Mg_{0.2}O_3$ electrolyte membranes for intermediate-temperature solid oxide fuel cells, J. Mater. Chem. A, **3** (2015) 7535–7553. https://doi.org/10.1039/C5TA01203A

60. Hwang C, Tsai C-H, Lo C-H, Sun C-H, Plasma sprayed metal supported YSZ/Ni–LSGM–LSCF ITSOFC with

nanostructured anode, J. Power Sources, **180** (2008) 132–142. https://doi.org/10.1016/j.jpowsour.2008.01.075

61. Hwang C, Tsai C-H, Yu J-F, Chang Ch-L, et al., High performance metal-supported intermediate temperature solid oxide fuel cells fabricated by atmospheric plasma spraying, J. Power Sources, **196** (2011) 1932–1939. https://doi.org/10.1016/j.jpowsour.2010.10.029

62. Tsai C-H, Hwang C, Chang C-L, Yu J-F, et al., Post-heat treatment pressure effect on performances of metal-supported solid oxide fuel cells fabricated by atmospheric plasma spraying, J. Power Sources, **197** (2012) 145–153. https://doi.org/10.1016/j.jpowsour.2011.09.018

63. Sun K, Zhang J, Jiang T, Qiao J, et al., Flash-Sintering and Characterization of $La_{0.8}Sr_{0.2}Ga_{0.8}Mg_{0.2}O_{3-\delta}$ Electrolytes for Solid Oxide Fuel Cells, Electrochimica Acta, **196** (2016) 487–495. https://doi.org/10.1016/j.electacta.2016.02.207

64. Guo W, Liu J, Zhang Y, Electrical and stability performance of anode-supported solid oxide fuel cells with strontium- and magnesium-doped lanthanum gallate thin electrolyte, Electrochimica Acta, **53** (2008) 4420–4427. https://doi.org/10.1016/j.electacta.2008.01.039

65. Guo W, Liu J, A novel design of anode-supported solid oxide fuel cells with Y_2O_3-doped Bi_2O_3, $LaGaO_3$ and La-doped CeO_2 trilayer electrolyte, J. Power Sources, **195** (2010) 8185–8188. https://doi.org/10.1016/j.jpowsour.2010.07.039

66. Guo W-M, Pei J-Y, Liang H-Y, Liu J, Preparation and Performance of Anode-supported $LaGaO_3$-based Electrolyte Solid Oxide Fuel Cells with Sm-doped CeO_2 Buffer Layers: Preparation and Performance of Anode-supported $LaGaO_3$-based Electrolyte Solid Oxide Fuel Cells with Sm-doped CeO_2 Buffer Layers, J. Inorg. Mater., **26** (2011) 685–690. https://doi.org/10.3724/SP.J.1077.2011.00685

67. Wang L-S, Li C-X, Li G-R, Yang G-J, et al., Enhanced sintering behavior of LSGM electrolyte and its performance for solid oxide fuel cells deposited by vacuum cold spray, J. Eur. Ceram. Soc., **37** (2017) 4751–4761. https://doi.org/10.1016/j.jeurceramsoc.2017.06.007

68. Kim K, Kim B, Son J, Kim J, et al., Characterization of the electrode and electrolyte interfaces of LSGM-based SOFCs, Solid State Ion., **177** (2006) 2155–2158. https://doi.org/10.1016/j.ssi.2006.02.011

69. Ha SB, Cho YH, Kang YC, Lee J-H, et al., Effect of oxide additives on the sintering behavior and electrical properties of strontium- and magnesium-doped lanthanum gallate, J. Eur. Ceram. Soc., **30** (2010) 2593–2601. https://doi.org/10.1016/j.jeurceramsoc.2010.05.007

70. Huang P, Horky A, Petric A, Interfacial Reaction between Nickel Oxide and Lanthanum Gallate during Sintering and its Effect on Conductivity, J. Am. Ceram. Soc., **82** (1999) 2402–2406. https://doi.org/10.1111/j.1151-2916.1999.tb02096.x

71. Ha SB, Cho YH, Ji H-I, Lee J-H, et al., Low-temperature sintering and electrical properties of strontium- and magnesium-doped lanthanum gallate with V_2O_5 additive, J. Power Sources, **196** (2011) 2971–2978. https://doi.org/10.1016/j.jpowsour.2010.11.082

72. Larregle SC, Baqué L, Mogni L, Effect of aid-sintering additives in processing of solid oxide fuel cells electrolytes by tape casting, Solid State Ion., **394** (2023) 116210. https://doi.org/10.1016/j.ssi.2023.116210

73. Fan S, Jin T, Zhang S, Luo X, et al., Effect of Li_2O Sintering Aid on Sintering Characteristics and Electrical Conductivity of LSGM Electrolyte for Solid Oxide Fuel Cell, J. Inorg. Mater., **37** (2022) 1087. https://doi.org/10.15541/jim20220086

74. Kumar M, Nesaraj AS, Raj IA, Pattabiraman R, Synthesis and characterization of $La_{0.9}Sr_{0.1}Ga_{0.8}Mg_{0.2}O_{3-\delta}$ electrolyte for intermediate temperature solid oxide fuel cells (ITSOFC), Ionics, **10** (2004) 93–98. https://doi.org/10.1007/BF02410313

75. Reis SL, Muccillo ENS, Influence of small amounts of gallium oxide addition on ionic conductivity of $La_{0.9}Sr_{0.1}Ga_{0.8}Mg_{0.2}O_{3-\delta}$ solid electrolyte, Ceram. Int., **44** (2018) 115–119. https://doi.org/10.1016/j.ceramint.2017.09.139

76. Wang J, Zhou D, Wang Y, Meng J, et al., Effect of sintering aid MoO_3 on the microstructure and ionic conductivity of ceria- and lanthanum gallate-based electrolytes, Phase Transit., **91** (2018) 1277–1288. https://doi.org/10.1080/01411594.2018.1494829

77. Wang Y, Zhou DF, Chen L, Xie ShK, et al., Improvement in the sintering and electrical properties of strontium- and magnesium-doped lanthanum gallate by MoO_3 dopant, J. Alloys Compd., **710** (2017) 748–755. https://doi.org/10.1016/j.jallcom.2017.03.323